Brain Tumor Progression Modeling - A Data Driven Approach

Christian Weber[1,3],Michael Götz[1], Bram Stieltjes[3],Joanna Polanska[4],Franciszek Binczyk[4,5] ,Rafal Tarnawski[5] ,Barbara Bobek-Billewicz[5], and Klaus H. Maier-Hein[1,2]

[1]Junior Group in Medical Image Computing, German Cancer Research Center, Heidelberg, Germany
[2]Medical and Biological Informatics, German Cancer Research Center, Heidelberg, Germany
[3]Quantitative Image-based Disease Characterization, German Cancer Research Center, Heidelberg, Germany
[4]Silesian University of Technology, Gliwice, Poland
[5]Maria Skodowska-Curie Memorial Cancer Center and Institute of Oncology, Gliwice, Poland

Abstract. Malignant gliomas are highly heterogeneous brain tumors with complex anisotropic growth patterns and occult invasion. Computational modeling of cell migration and proliferation has been subject of intensive research aiming at a deeper understanding of the tumor biology and the ability to predict growth and thus improve therapy. However, current modeling techniques follow a generative approach and make strong assumptions about underlying mechanisms. The tumor is so far treated as homogeneous entity with behavioral parameters extrapolated from previous longitudinal image information.
We present a novel way of approaching this problem by employing data driven, discriminative modeling techniques that learn relevant features from observed growth patterns and are able to make meaningful predictions solely on basis of local and regional tissue characteristics at one given point in time.
We demonstrate superior performance of the proposed discriminative method (DICE score 83) compared to the state of the art generative approach (DICE score 72) on six patients and a total of nine different time intervals. Our approach can help estimating occult invasion as well as it can advance our understanding of the tumor biology and lead to valuable predictions of tumor growth patterns that could guide and improve radio therapy.

1 Introduction

Malignant gliomas are biologically heterogeneous primary brain tumors with anisotropic progression at variable rates. A major problem complicating therapy decisions is the invisible invasion margin of these tumors, that is tumor cells that migrate into the healthy brain but do not yet cause detectable signal changes in MR. Computational modeling of cell migration and proliferation can help estimating this occult invasion as well as it can aid our understanding of biological factors in heterogeneous tumors. Treatment procedures in radio-therapy usually employ an isotropic 2 cm safety margin with brain tumors to account for occult invasion. Patient specific predictions of tumor growth patterns could guide and improve therapy by adapting to these anisotropic growth patterns.

Current techniques follow a generative approach and directly or indirectly model the diffusion of tumor cells by employing the diffusion reaction equation or derived diffusion-based distance metrics.

Swanson *et al.* first modeled diffusing tumor cells in dependence on the underlying tissue type following the observation that glial cells show higher motility in white matter than in

gray matter [10]. This idea has later been extended by studies that derive the so called Tumor Diffusion Tensor (TDT) from the Diffusion Tensor Image (DTI), thereby taking into account the local fiber orientation [2–4, 9]. A quantitative evaluation of glioma growth simulations on real patient data has so far only been performed by two studies [5, 9]. For a given time point and given gross tumor volume (GTV), Mosayebi *et al.* estimate an infinite set of possible occult tumor invasion margins with varying distances from the tumor by means of a diffusion-based distance metric. In order to choose one prediction from the set of margins for their evaluation, the authors circumvent the problem of model instantiation by choosing the optimal contour that matches the volume gain of the future contour that is to be predicted. For the thus chosen optimal contour the authors reported a mean Jaccard score of 59. As input, the algorithm requires a segmentation of the ventricular system, falx cerebri and tentorium cerebelli, which are used as growth barriers. Stretton *et al.* use a traveling wave formulation of the diffusion-reaction equation to simulate tumor progression. In order to predict a subsequent time step, the model requires two consecutive time steps for the initialization of the individual progression rate. Unfortunately, the study included only one malignant glioma for which the authors reported a root mean square error of 6mm considering this prediction.

A major shortcoming of the previously proposed techniques is that they treat the tumor as one homogeneous mass, imposing rather strong assumptions on its behavior based on only small fractions of the available image information. They cannot account for tumor progression along selective fiber tracts and do not account for the biological heterogeneity within the tumor. Furthermore, in order to instantiate the models, longitudinal image information and time-consuming segmentation of gray and white matter and other anatomical structures are so far indispensable.

We propose a novel discriminative approach for tumor progression modeling that allows for the incorporation of an arbitrary number of different sources of information such as local tissue characteristics and regional context. The relevant aspects are identified and weighted in a data-driven learning step that analyses growth patterns in an annotated database. Tumor progression is then predicted for unseen cases on basis of a single time point without the need of parameter estimation or any structural annotations. We demonstrate the advantages of our method over the state of the art using a dataset of nine cases.

2 Methods

2.1 Patient Data

The data set consists of longitudinal data from six patients with grade IV glioblastoma showing significant re-growth after initial resection. A total of nine acquisition pairs derived from these patients are used in this study. T1-weighted with contrast agent,T2-FLAIR, and DTI imaging is available for each time step. Resolutions are $0.625 \times 0.625 mm^2$ in plane, 6mm spacing for T1 and T2, and $1.796 \times 1.796 mm^2$ in plane, 5.2mm spacing for DTI. Images have been co-registered and resampled to $1 \times 1 \times 3mm$ separately for each patient using the Medical Imaging Interaction Toolkit (MITK) [6]. The GTV has been manually segmented in all time steps with an iterative refinement procedure based on Tumor Progression Mapping (TPM) in order to ensure the temporal consistency of the segmentations [11]. The time spans between the image pairs lay between 158 and 251 with an average of 183 days.

2.2 Previous generative approach

Most simulation approaches model cell spread using the diffusion-reaction equation

$$\frac{\partial c}{\partial t} = \nabla(\boldsymbol{D}\nabla c) + p(c) \tag{1}$$

where c denotes the concentration of tumor cells, $\boldsymbol{D}$ the diffusion tensor and $p(\cdot)$ the reaction term that models cell proliferation. In [3] Konukoglu *et al.* show that the proliferation rate can be fixed and diffusion speed used to adapt the model to a patient specific case. In [9] Stretton *et al.* show that using TDTs derived from patients DTIs perform superior to DTI atlas or white-matter derived TDTs. We implemented the simulation using a fixed proliferation rate with patient specific TDTs constructed as follows:

$$\boldsymbol{TDT}(x) = \begin{cases} \boldsymbol{D}_w(x) & \text{if FA}(x) > .2 \\ d_g \boldsymbol{I} & \text{else} \end{cases} \tag{2}$$

with d_g representing the diffusion constant that is used in gray matter; the FA value is used to discriminate against gray matter. $\boldsymbol{D}_x$ is normalized by the highest eigenvalue in white matter.

The reported ratio between diffusivity within grey matter and white matter greatly varies in literature, we tested several values and found best overall performance for a maximal diffusivity within white matter being 20 times the diffusivity within grey matter. This parameter is of course obtained as an optimum for all patients and therefore fix in the model as our main interest is to investigate the general prediction accuracy on unseen cases.

2.3 Novel Discriminative Approach

We apply random forests and manually annotated training data to learn the growth patterns of malignant gliomas [1]. Given the image data and a segmentation of the current tumor margin, we aim at classifying the voxels that will transform to tumor versus the ones that will remain unaffected. The relevant criteria for this decision are learned from data rather than imposed by a generative model.

For a pair of multi-modal images (I^t, I^{t+1}) from two time steps t and t+1, each voxel v^t in I^t is represented by a feature vector $\boldsymbol{x} \in \mathrm{X}$ and a label $y \in \mathrm{Y}$, where Y consists of two labels: 'future tumor', i.e. the corresponding voxel v^{t+1} in I^{t+1} is labeled tumor and 'future non-tumor', i.e. the corresponding voxel v^{t+1} in I^{t+1} is labeled non-tumor. From training data a classifier is then build that estimates the probability $P(x, y)$ for previously unseen data. The label assigned to a voxel is the label with the highest probability for the corresponding feature vector

$$y = \arg\max_y P(\boldsymbol{x}, y) \ . \tag{3}$$

The splitting function for each node in the random forests is a threshold on a single feature. We use the Gini-index to determine the optimal threshold. Forest size is set to 1000 and maximal tree depth is limited to 6 to ensure good generalization. In order to supply the classifier with meaningful information, the vector $\boldsymbol{x}$ consists of features that represent 1) the local tissue characteristics, 2) the regional context of the voxel, and 3) diffusion-based distance measures as described in section 2.2.

Features representing local tissue characteristics We include normalized T1, T2-FLAIR, and DTI derived measures (FA, MD, RD, AD, b0) with and without the application of free-water elimination as measures describing the local tissue configuration [7].

Features representing regional context The most straight-forward way to describe the regional relation of any voxel is using the euclidean distance of a voxel v^{target} to the initial GTV. However, biological heterogeneity and e.g. preferential growth along white matter tracts cause tumor growth to be highly anisotropic. Therefore the likelihood of tumor progression towards a specific voxel v^{target} outside the initial GTV cannot be fully represented by such simple distance measures.

To account for this, we introduce novel connectedness measures that are inspired by the idea of fuzzy connectedness maps [8].

The connectedness $s(\cdot,\cdot)$ between adjacent voxels v_l and v_k incorporates the diffusion tensor $\boldsymbol{D_l}$ at location v_l and an arbitrary scalar map value $f(\cdot)$. Let vector $\boldsymbol{r}$ point from voxel position v_l to v_k. The similarity of adjacent voxels is then defined as

$$s(v_l, v_k) = \left(\|\boldsymbol{D_l} \cdot \boldsymbol{r}\|_2\right)^{-1} \cdot \left(e^{|f(v_k)-f(v_l)|} - 1\right) \tag{4}$$

where $\|\boldsymbol{D_l} \cdot \boldsymbol{r}\|_2$ denotes the magnitude of the projection of vector $\boldsymbol{r}$ unto the diffusion tensor $\boldsymbol{D_l}$. This formulation allows the computation of differently weighted distance maps based on different feature maps $f(\cdot)$ such as FA, MD and RD. The connectedness of two non-adjacent voxels v^{GTV} and v^{target} is determined considering all possible paths between these voxels; each possible path $i : v_0^{GTV}, v_1, \ldots, v_n^{target}$ is assigned the cumulated value of differences between adjacent voxels along this path:

$$s(i) = \sum_{j=0}^{n-1} s(v_j, v_{j+1}) \tag{5}$$

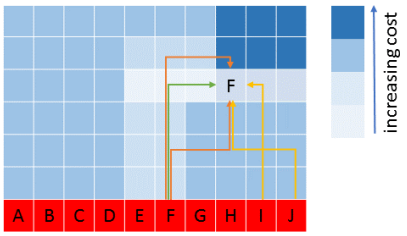

Fig. 1: Feature propagation. Red denotes the tumor border. The letters represent features that describe the tumor at that location. Blue values represent the cost for traveling through a given voxel (to simplify visualization they are assumed to be invariant to the direction), light values depict low costs, dark ones high costs. The arrows depict possible paths from the tumor outline to v^{target}. The green path has lowest cumulative cost, which is why it is chosen to propagate its originating feature value.

The path i^* with the minimum value is then chosen as the path with the highest connectedness between the voxels. After identifying this path, the cumulative connectedness value $s(i^*)$

as well as the local features at v^{GTV} (the origin of the path, c.f. Fig. 1) are used as features in the feature vector of v^{target}.

Diffusion-based distance measure According to the above described generative approach an additional feature map is computed using the un-thresholded result of a diffusion process. It is to be noted that this generative map is computed with a fixed parameter set, that is, no patient specific parameters are needed to compute this feature.

3 Results

We applied the above described methods to all data sets (acquisition pairs), training the random forests in a leave-one-patient-out protocol. We then used these trees to predict on the data of the unseen patient. We calculated the Dice score and Jaccard index of the predictions on basis of I^t and the tumor segmentation in I^{t+1}. These scores are only computed on newly grown tumor, voxels already marked as tumor at time point t were not considered in the evaluation. We also calculated the RMSE between the two corresponding outlines.

To compare our method to the current state of the art, we used the diffusion model described in section 2.2 (c.f. Fig. 2). Optimal growth rates have been determined via a leave-one-patient-out protocol.

Fig. 3 depicts the RMSE of the diffusion model in a range of sensitivities between 45% and 95% that were estimated by varying the growth rates. The approach shows an increasing RMSE with increasing sensitivity. The maximum RMSE corresponds to the findings of Stretton *et al.* who reported RMSE values of about 6mm [9]. The RMSE using the novel discriminative approach is constantly below 3mm, but produces one outlier with an extremely low sensitivity.

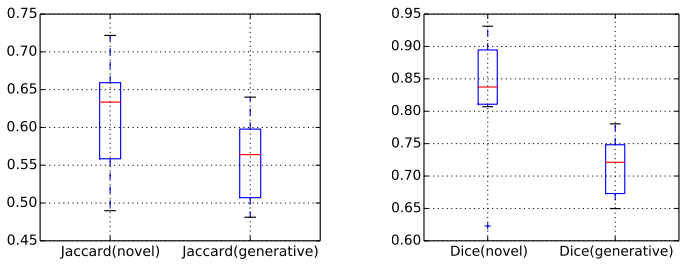

(a) (b)

Fig. 2: Statistical comparison of the two methods. The novel discriminative random forest based approach (novel) compared with previous generative approach (generative).

Fig. 4 depicts exemplary results for both methods. Our method (yellow outline) closely follows the tumor outline in I^{t+1} (red outline). In cases where it under- or overestimates the spiky extensions of the tumor, it still mimics the specific growth pattern while the diffusion approach provides a rather balloon-like outline in these regions.

Furthermore, these examples demonstrate the ability of the proposed method to infer natural growth barriers such as the ventricles directly from the training samples (c.f. Fig. 4).

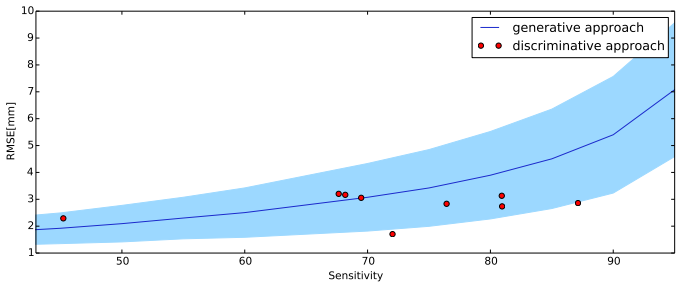

Fig. 3: RMSE versus Sensitivity: Solid line denotes mean RMSE over all 9 predictions for the respective sensitivities, the area denotes the standard deviation. The red dots are results using our method. It can be seen that for increasing sensitivities the diffusion model becomes less accurate, while our method remains accurate.

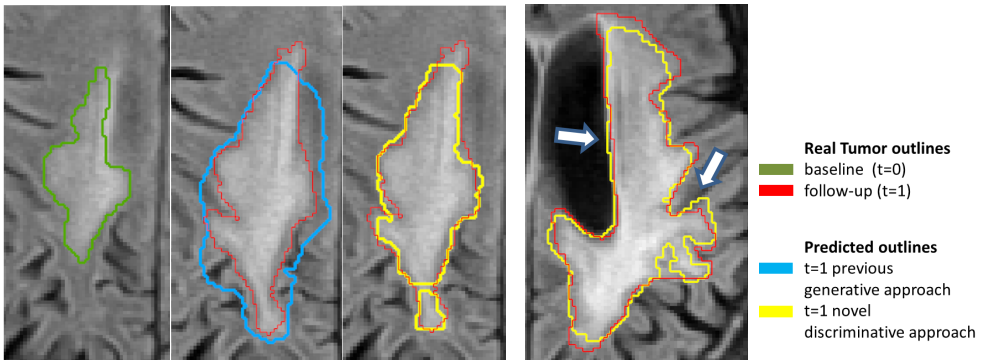

Fig. 4: Overlay of tumor outlines on T2-FLAIR images. Intial contours from I^t (green), ground truth of prediction from I^{t+1} (red), the novel discriminative approach (yellow), and the previous generative approach (blue) are shown. (a)-(c) depict the different outlines. (a) shows the initial contour on T2-FLAIR at $t = 0$. (b) depicts the overlay of the ground truth from I^{t+1} and the prediction of the generative approach on T2-FLAIR at $t = 1$. (c) displays the overlay of the ground truth from I^{t+1} and the prediction our discriminative approach on T2-FLAIR at $t = 1$. (d) demonstrates the ability of our approach to infer natural growth barriers such as ventricles and sulci (see arrows) directly from the training samples.

4 Discussion & Outlook

We proposed a novel discriminative approach to learn and predict tumor growth patterns. We evaluated this method on nine time intervals and compared it to the ground truth as well as to the state of the art generative approach. The assessment of the generative approach (Jaccard index of 56, RMSE of around 6-7mm) is in very good agreement with the currently available studies on quantitative evaluation of tumor progression modelling or invasion margin estimation on real patient data (Mosayebi *et al.*: Jaccard index of 59 [5], Stretton *et al.*: RMSE of 6mm [9]). The newly proposed discriminative approach clearly outperforms the state of the art technique, given the setup without manually marked growth barriers.

In comparison to generative modelling, our discriminative approach has several intrinsic advantages. It allows for straight-forward inclusion and combination of a variety of different features. The behavior of the tumor including the consideration of natural growth barriers and the preferential growth direction along fibers is learned from the data. This enables an accurate and patient-specific prediction in a clinical routine without adding the need of additional time consuming manual annotations of growth barriers or additional longitudinal image data to estimate growth parameters. While the current generative models seem to cover some important aspects of the growth patterns of malignant gliomas, the higher predictive value of our approach suggests that the underlying mechanisms are more complex and more adequately represented by richer sets of features beyond the diffusion tensor and FA. The presented approach can make use of the full set of information available in the different MR modalities and will potentially further benefit from the development of advanced feature sets. Furthermore apart from predicting binary tumor outline the approach associates each voxel with a probability of becoming tumor which can guide the dose application in radio therapy.

Naturally the predictive value of the proposed approach depends on the representativity and size of the training data set. Learning from observed data, though more flexible by design, can pose a potential weakness since its performance depends on the data set that is used to train it. Such a method performs less good on cases that are not well covered by the training data base, such as one outlier in Fig. 3 for which only a very low sensitivity could be achieved. In such cases where observed samples are rare a generative model may yield better results.

In the future, we plan on extending our data base in order to cover a higher variety of patterns that can be successfully predicted. Also, we want to follow up on a highly interesting question that arises from our results: the analysis of variable importance measures in order to learn more about the determining factors in malignant glioma growth. This might lead to a better understanding of the underlying mechanisms in the progression of high grade gliomas.

Funding: This work was carried out with the support of the German Research Foundation (DFG) within project R01, SFB/TRR 125 Cognition-Guided Surgery.

References

1. Leo Breiman. Random forest. *Machine Learning*, 45:1–35, 1999.
2. Saâd Jbabdi, Emmanuel Mandonnet, Hugues Duffau, Laurent Capelle, Kristin Rae Swanson, Mélanie Pélégrini-Issac, Rémy Guillevin, and Habib Benali. Simulation of anisotropic growth of low-grade gliomas using diffusion tensor imaging. *Magnetic resonance in medicine : official journal of the Society of Magnetic Resonance in Medicine / Society of Magnetic Resonance in Medicine*, 54(3):616–24, September 2005.

3. Ender Konukoglu, Olivier Clatz, Bjoern H Menze, Bram Stieltjes, Marc-André Weber, Emmanuel Mandonnet, Hervé Delingette, and Nicholas Ayache. Image guided personalization of reaction-diffusion type tumor growth models using modified anisotropic eikonal equations. *IEEE transactions on medical imaging*, 29(1):77–95, January 2010.
4. Anitha Priya Krishnan, Delphine Davis, Paul Okunieff, and Walter O'Dell. Random walk model based on DTI for predicting the microscopic spread of gliomas. *2008 5th IEEE International Symposium on Biomedical Imaging: From Nano to Macro*, pages 891–894, May 2008.
5. Parisa Mosayebi, Dana Cobzas, Albert Murtha, and Martin Jagersand. Tumor invasion margin on the Riemannian space of brain fibers. *Medical image analysis*, 16(2):361–73, February 2012.
6. Marco Nolden, Sascha Zelzer, Alexander Seitel, Diana Wald, Michael Müller, Alfred M Franz, Daniel Maleike, Markus Fangerau, Matthias Baumhauer, Lena Maier-Hein, Klaus H Maier-Hein, Hans-Peter Meinzer, and Ivo Wolf. The Medical Imaging Interaction Toolkit: challenges and advances : 10 years of open-source development. *International journal of computer assisted radiology and surgery*, 8(4):607–20, July 2013.
7. Ofer Pasternak, Nir Sochen, Yaniv Gur, Nathan Intrator, and Yaniv Assaf. Free water elimination and mapping from diffusion MRI. *Magnetic resonance in medicine : official journal of the Society of Magnetic Resonance in Medicine / Society of Magnetic Resonance in Medicine*, 62(3):717–30, September 2009.
8. Azriel Rosenfeld. Fuzzy digital topology. *Information and Control*, 40(1):76–87, January 1979.
9. E Stretton and E Geremia. Importance of patient DTI's to accurately model glioma growth using the reaction diffusion equation. *International Symposium on Biomedical Imaging: From Nano to Macro*, 1130(32):5–8, 2013.
10. KR Swanson, EC Alvord, and JD Murray. A quantitative model for differential motility of gliomas in grey and white matter. *Cell proliferation*, 33:317–329, 2000.
11. Christian Weber, Bram Stieltjes, Joanna Polanska, Franciszek Binczyck, Rafal Tarnawski, Barbara Bobek-Billewicz, Timo Rodi, Sebastian Regnery, and Klaus H Fritzsche. Tumor progression mapping: An intuitive visualization of glioblastoma progression in mr follow-ups. *Proc. Annual Meeting ISMRM, Mailand*, 2014.